Analysis of Shorthorn Sculpin Antifreeze Protein Stereospecific Binding to (2 −1 0) Faces of Ice

A. Wierzbicki,* M. S. Taylor,* C. A. Knight,# J. D. Madura,* J. P. Harrington,* and C. S. Sikes§
*Department of Chemistry, University of South Alabama, Mobile, Alabama 36688; #National Center for Atmospheric Research, Boulder, Colorado 80307; §Department of Biological Sciences, University of South Alabama, Mobile, Alabama 36688 USA

ABSTRACT In this paper we report the results of our studies on the stereospecific binding of shorthorn sculpin antifreeze protein (AFP) to (2 −1 0) secondary prism faces of ice. Using ice crystal growth and etching techniques together with molecular modeling, molecular dynamics, and energy minimization, we explain the nature of preferential binding of shorthorn sculpin AFP along the [1 2 2] direction on (2 −1 0) planes. In agreement with ice etching studies, the mechanism of preferential binding suggested by molecular modeling explains why the binding of shorthorn sculpin AFP occurs along [1 2 2] and not along its mirror symmetry-related direction [−1 −2 2] on (2 −1 0). This binding mechanism is based on the protein-crystal surface enantioselective recognition that utilizes both α-helical protein backbone matching to the (2 −1 0) surface topography and matching of side chains of polar/charged residues with specific water molecule positions in the ice surface. The mechanisms of winter flounder and shorthorn sculpin antifreeze binding to ice are compared.

INTRODUCTION

Some organisms are able to survive in environments with temperatures below the freezing point of water by producing antifreeze proteins (AFP) or antifreeze glycoproteins (AFGP) (Davies and Hew, 1990; Cheng and DeVries, 1991; Hew and Yang, 1991; Duman et al., 1993). These molecules prevent potential damage from freezing in a noncolligative fashion by binding to specific planes of ice crystals. This adsorption results in the cessation of ice growth from melt and a nonequilibrium depression of the freezing point. The freezing point depression depends upon AFP concentration and is believed to operate by the Kelvin effect (Raymond and DeVries, 1977; Knight et al., 1991).

The first AFPs discovered, type I AFPs, are right-handed α-helical molecules of around 40 residues and high alanine content. Etching studies (Knight et al., 1991) performed on three type I AFPs revealed highly stereospecific binding of type I AFPs from winter flounder and Alaskan plaice to (2 0 1) and from shorthorn sculpin to (2 −1 0) crystallographic planes of ice. This binding was not only selective with respect to indicated planes, but also highly directional along a ⟨1 2 2⟩ vector common for all three types of AFPs. Knight et al. (1991) suggested that the match of the threonine residue spacing in the winter flounder AFP with the 16.7 Å spacing of ice along the ⟨1 2 2⟩ direction was the key to explaining the adsorption. This was used by Wen and Laursen (1992), Madura et al. (1994), and Laursen et al. (1994) to elucidate the preferential binding to ice of the L and D forms of winter flounder antifreeze.

The polar and charged residues of the shorthorn sculpin α-helix do not have an obvious repetitive motif that can be matched with the ice lattice periodicity. In this study we use the ice etching method, molecular modeling, and molecular dynamics to elucidate the stereospecificity of preferential binding of shorthorn sculpin along the [1 2 2] direction on the (2 −1 0) plane of ice and to understand why it adsorbs along the [1 2 2] but not the [−1 −2 2] direction on the (2 −1 0) plane.

MATERIALS AND METHODS

Experimental

Knight et al. (1991) used 0.015 mg/ml of natural, shorthorn sculpin antifreeze to produce the etch pattern that enabled the adsorption plane and adsorption alignment to be deduced. That experiment was repeated for this work, using a more concentrated 0.07 mg/ml solution of synthesized material with the same amino acid sequence (MacroMolecular Resources, Colorado State University, Fort Collins, CO). A more concentrated solution was used in this study to produce clear etching patterns suitable for photography. Concentrations as low as 0.015 mg/ml of synthetic material were equally sufficient for the determination of adsorption plane. Single-crystal, oriented ice hemispheres were grown from the solution from the end of a cold finger inserted into the surface of the solution. The crystals were oriented with a prism plane normal to the axis of the cold finger (parallel to the base of the hemisphere), so that all surface orientations were represented on the curved surface of the hemisphere. The AFP molecules adsorb at the growing surface where the orientation is correct for adsorption, and are incorporated into the growing ice crystal only in those regions; elsewhere they do not adsorb and are rejected. With extremely diluted solutions the AFP does not influence the growth rate and consequently does not influence the hemisphere shape. With increasing solution concentration, however, the hemispheres develop flattened areas where the adsorption occurs because of the slowing of the growth. In either case, presence of the AFP within the ice is detected very simply by scraping the hemisphere surface and then allowing it to evaporate slowly. Pure ice develops a highly polished, completely rounded surface, but in the sectors where the AFP has been incorporated the evaporation of the ice concentrates AFP at the surface, and the surface gets a glazed "ground-glass" appearance. This etching procedure was performed using different concentrations of the peptide.

Received for publication 23 June 1995 and in final form 21 March 1996.
Address reprint requests to Dr. Andrzej Wierzbicki, Department of Chemistry, University of South Alabama, Mobile, AL 36688. 334-460-7436; 334-460-7359; wierzb@moe.chem.usouthal.edu.

0006-3495/96/07/08/11 $2.00

Modeling

All computational operations were performed on an SGI INDIGO^2 workstation with an R4400 150 MHz processor and EXTREME graphics. For modeling purposes, two 31.2 Å × 79.3 Å × 6.9 Å blocks were extracted from a secondary prism face (2 −1 0) of a simulated ice-Ih crystal slab, each block containing 738 TIP3 (Jorgensen et al., 1983) water molecules. The ice slabs were constructed from the asymmetric fractional coordinates of ice using CERIUS^2 (CERIUS^2, Version 1.0 of molecular modeling software for materials research from Molecular Simulations, Inc., of Burlington, MA, and Cambridge, England). Once the slab was prepared, the hydrogen positions of ice were randomized by running a 5-ps, 2000 K dynamics simulation in which the oxygen positions were held fixed, followed by 500 steps of steepest descent minimization (Madura et al., 1994) using CHARMm 22 (CHARMm 22 molecular modeling software from Molecular Simulations). The blocks were cut as follows: with the long axis of the first block extended along the [1 2 2], whereas the second slab long axis extended in the [−1 −2 2] direction, the mirror image of [1 2 2]; each ice block contained 738 water molecules. A shorthorn sculpin (*Myoxocephalus scorpius*) AFP model was constructed from the following 42-residue sequence (Knight et al., 1991; Cheng and DeVries, 1991):

MDGETPAQKAARLAAAAAALAAKTAADAAAKA

AAIAAAAASA

using QUANTA 4.0 (QUANTA 4.0 molecular modeling software from Molecular Simulations). The AFP α-helix structure was modeled on each ice block by first orienting the helix parallel (±5°C) to the long edge of the block. The first set of modeling trials was performed along [1 2 2] and the second along [−1 −2 2]. Because each of the ice blocks is superimposable on itself when rotated 180°C, the two possible orientations of the protein C and N termini with respect to [1 2 2] and [−1 −2 2] vectors were equivalent. The hydrophilic AFP surface was presented to the ice surface in such a way that structural reciprocation and hydrogen bonding were maximized as described below in the Results. Each modeling trial was subjected to a series of energy minimizations consisting of 500 steps of steepest descent followed by 500 steps of ABNR minimization procedure of CHARMm 22, with water oxygen atoms remaining fixed and allowing for the rigid-body rotations of water molecules. A binding energy was then calculated by subtracting the sum of the individual ice and protein energies from the energy of the minimized protein/ice system. Each minimized system was analyzed for structural fitting and hydrogen bonding.

Molecular dynamics

A NVE molecular dynamics simulation was performed on a system consisting of a single 42-residue type I AFP solvated in a periodic box of TIP3 water molecules. The starting protein structure used was an ideal α-helix structure of the shorthorn sculpin. Polar hydrogens were added to the protein using QUANTA/CHARMm 4.0 (QUANTA/CHARMm 4.0 molecular modeling software from Molecular Simulations). The protein was placed in a 90 × 36 × 36 Å^3 slab of water, and all water molecules with oxygens within 2.3 Å of the solute were removed.

The solvated protein, consisting of 11,297 atoms, was initially subjected to 200 steps of steepest descent energy minimization to relax the protein-water interactions by holding the protein fixed and allowing the waters to freely move. This was followed by another 200 steepest descent energy minimization steps in which the solute was free to move and the waters were held fixed. Final 200 steepest descent energy minimizations were done in which both the protein and water were free to move. At the end of the minimization the RMS gradient was 1.896 and the total energy for the system was −45,501 kcal/mol. The system, with no constraints, was then subjected to 10 ps of thermalization, increasing the temperature from 0 K to 300 K in 6 K increments, followed by 50 ps of equilibration. Finally, data were collected for 84 ps, with coordinate, velocity, and energy files being saved every 0.05 ps. A nonbonded cutoff of 12 Å was used in the calculations, and the nonbonded list was updated every 25 steps. The electrostatic and van der Waals potential energy terms were gradually switched to zero over the range of 9.0 to 11.0 Å. All dynamics calculations and dynamics analysis were performed using CHARMM 22 (Brooks et al., 1983).

RESULTS AND DISCUSSION

Experimental

Fig. 1 shows an etched hemisphere surface grown from a solution concentration of about 0.07 mg/ml of the peptide. The photo shows the rounded surface of the hemisphere after its flat side was frozen to a dull black metal plate. The hole where the end of the cold finger had been was also filled with a black cap frozen into ice. These dull black surfaces prevent reflections off the far side of the ice during photography. A prism plane is parallel to the plane of the photo, and the parallel, up-and-down oriented, bright lines and line segments are air bubbles oriented parallel to the crystallographic *c* axis. These bubbles are faceted, and the sculpin antifreeze is the only one that we have examined that produces this feature in hemisphere growth. At this concentration there exists a distinct flattening of the ice surface where the etching is seen, although it is not visible in the photograph because of the angle. Two large, distinct etched regions are visible at the right and left sides of the photo. The orientation of the tangent plane to the surface at the centers of the etched regions is taken to reveal the "adsorption plane," and the elongation direction of the etched regions on the curved surface is normal to the AFP alignment direction on the adsorption plane. The justification for the alignment is found in the work of Knight et al. (1991). The edges of the etched areas are rather irregular, and the etching intensity is also irregular, especially as the etching commences. The photograph was taken after about 20 h of etching.

Rotating the ice hemisphere 30°C about the *c* axis (about a N-S line in Fig. 1) places the adsorption plane (2 −1 0)

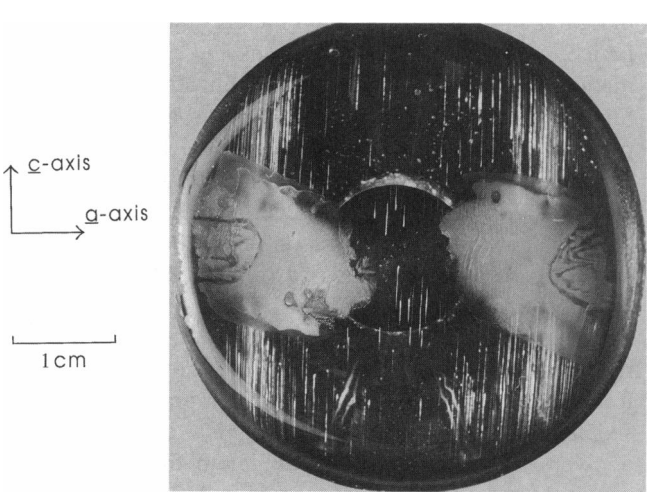

FIGURE 1 Etching pattern on single-crystal hemisphere grown from 0.07 mg/ml solution of shorthorn sculpin AFP, oriented as shown. The bright lines are air bubbles, oriented parallel to *c* axis.

normal to the direction of the view (if the hemisphere were an entire sphere this would move one or the other of the etched regions shown in Fig. 1 into the center). Viewed at this angle, the elongation of the etched regions can be measured. Now if the circular outline is a compass face, with north at the top, the elongation of the etched regions is toward the ESE and WNW, as it already appears in Fig. 1. The eastern azimuth would be 118° if the AFP orientation were ideal along [1 2 2], as reported by Knight et al. (1991). Several new independent estimates were made of this angle, which the shape of the etched region does not define with precision, and they ranged between 118° and 110°. This may or may not be a significant deviation from the low index direction, but we note that because the shorthorn sculpin AFP is not exactly periodic, there is no strong reason for this alignment on the ice to be an exactly rational crystallographic direction.

Just like the winter flounder AFP etching experiment (Knight et al., 1991), a remarkable feature of shorthorn sculpin etch pattern is that its symmetry is different from that of ice, lacking a mirror plane of symmetry. If present it would give each of the etched regions a "fat X" shape.

Modeling

Different AFP binding positions were tested via rotational and translational movements of the protein as well as torsional manipulations of side chains to provide the best possible initial configuration for energy minimization. More than 50 trials were conducted along each direction, [122] and [−1 −2 2], to provide sufficient initial configuration sampling. Modeling of the shorthorn sculpin AFP on (2 −1 0) along the [1 2 2] direction of ice yielded a binding energy of −608 kcal/mol. For each trial, the same very favorable structural match was achieved with the formation of multiple hydrogen bonds. Along the mirror image direction [−1 −2 2], shorthorn sculpin AFP binding energy yielded −530 kcal/mol. Inspection of binding in this direction revealed a marginal structural fit between the AFP and the ice crystal lattice, with different AFP positions and side-chain conformations being achieved during minimization for each trial. Structural and binding energy data strongly indicate the preferential binding of shorthorn sculpin AFP along the [1 2 2] direction of the (2 −1 0) plane. In fact, the binding along [−1 −2 2] on (2 −1 0) is energetically comparable to binding at random orientation on this plane. Results from a set of six random orientations of the AFP on (2 −1 0) produced a minimum energy of binding of −524 kcal/mol.

To understand why one of these two mirror symmetry-related orientations on (2 −1 0) is preferred over the other, it is useful to examine the specific topography of (2 −1 0) secondary prism planes. For a hexagonal ice crystal lattice, a given (2 −1 0) plane is parallel to the *c* axis and is perpendicular to an *a* axis (a_1 axis in Miller-Bravais notation). Prominent along the (2 −1 0) face are deep periodic half-hexagonal grooves parallel to the *c* axis (best seen in Fig. 4). The surface also shows regular rows of open tunnels along the *b* and −(*a* + *b*) directions (a_2 and a_3 axis in Miller-Bravais notation), which intersect (2 −1 0) at angles of 60° from normal to the surface, to form a pattern of alternating convex and concave bent hexagons or ice cages (Fig. 2 *a*). For the sake of brevity we will call these repetitive openings on the ice surface *a* axis cages. Fig. 2 *b* shows that although [1 2 2] and [−1 −2 2] are related by mirror symmetry, they are not superimposable. Thus an asymmetric chiral molecule would be expected to have different interactions with the ice surface when oriented along the two directions.

The shorthorn sculpin AFP is a heterogeneous, alanine-rich peptide with predominantly α-helical secondary structure. The hydrophilic side of this amphipathic protein displays several different polar and charged groups, defining a binding surface that is not clearly repetitive (Fig. 3). Unlike most type I AFPs, shorthorn sculpin AFP contains no repeats of the 11-residue sequence T A A N/D $(A)_7$. Repeat spacing of threonines has been implicated in winter flounder AFP binding based on structural complementarity and hydrogen bonding capability with respect to ice. An alternative spacing, however, occurs along the hydrophilic surface of many shorthorn sculpin species AFPs, primarily involving charged residues such as lysines (K). In the protein used for this study, K9 and K31 are 33.8 Å (22 residues) apart, whereas R12 and K23 are 16.9 Å (11 residues) apart. These distances are nearly exact multiples of the 16.7 Å spacing of the (2 −1 0) ice surface along the [1 2 2] and [−1 −2 2] vectors, indicating that the four basic residues instead of threonines may form the critical, specific hydrogen bonds for adsorption. This binding scheme is further supported by the fact that these amino acids extend lengthy side chains from the hydrophilic surface and are therefore probably the first to interact with ice. The two threonines contained in this shorthorn sculpin AFP are separated by 29.4 Å, showing less potential to dictate specific binding of the protein to ice. Their possible role in binding, however, will be discussed later.

Modeling of the shorthorn sculpin oriented along [1 2 2] revealed an obvious complementarity between the binding-surface residues and the ice topography such that the protein side chains could be easily accommodated by the *c* axis grooves and the *a* axis cages (Fig. 4, *right*). The strongest binding resulted when the K9 and K31 side chains with staggered low energy methylenes extended from the side of the protein down into *c* axis grooves and into the openings of the cages formed by the *a* axis. The 33.8 Å spacing of K9 and K31 provided for nearly identical positioning of the two residues (two *c* grooves apart) within the ice lattice, allowing for the accommodation of the bulky lysine side chains. Along the opposite side of the protein, R12 and K23 were accommodated in a similar fashion. Taken together, the binding face residues (shown in Fig. 3) compose a surface that fits the ice topography, with side chains within *c* axis grooves and the openings of the *a* axis cages and a noticeable lack of side-chain strain. The regular grouping of these side chains and the intermittent gaps between them allowed

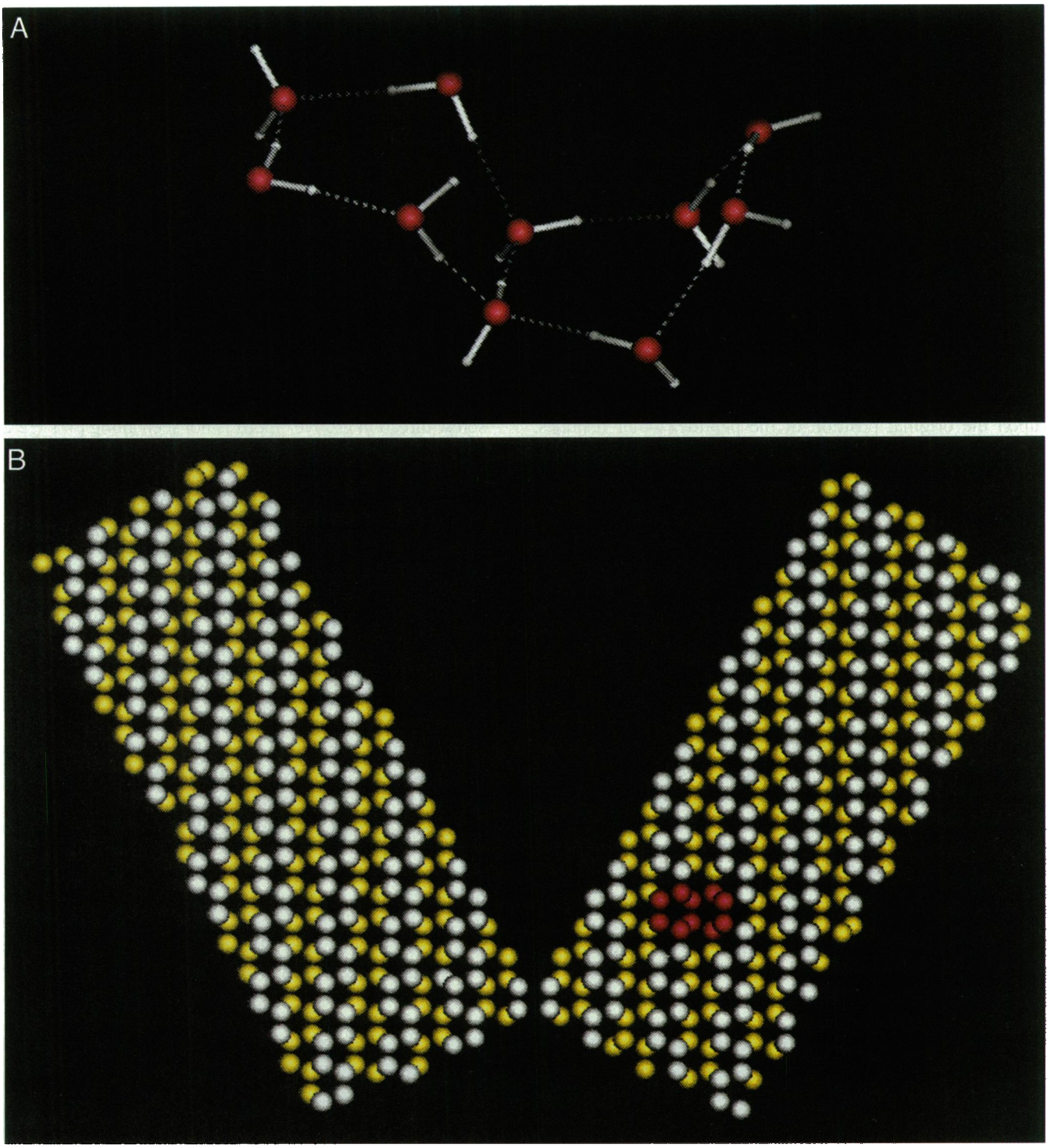

FIGURE 2 (*a*) Perspective view of the top fragment of (2 −1 0) ice surface topography (shown in red in *b*). Each distorted hexagon presents an opening to *a* axis cages that enter the (2 −1 0) surface at 60° to the surface normal. The trough at the right is a portion of one of grooves parallel to the *c* axis. (b) Side-by-side view of the two (2 −1 0) surface slabs cut along [1 2 2] (*right*) and [−1 −2 2] (*left*) mirror related vectors with *c* axes (*vertical axes in the plane of the picture*) aligned parallel to each other. The upper-layer oxygens are indicated in white, and the lower-layer oxygens are yellow. Note the position of *c* axis grooves that are parallel to the *c* axis in each of the slabs.

for a contoured fit of the protein. The side-chain conformation of the peptide shows little change upon adsorption to ice, especially for K9 and K31.

The accommodation to ice in the [−1 −2 2] direction is quite different. K9 and K31 are well accommodated into *c* axis grooves because of their 33.8 Å spacing, but they no

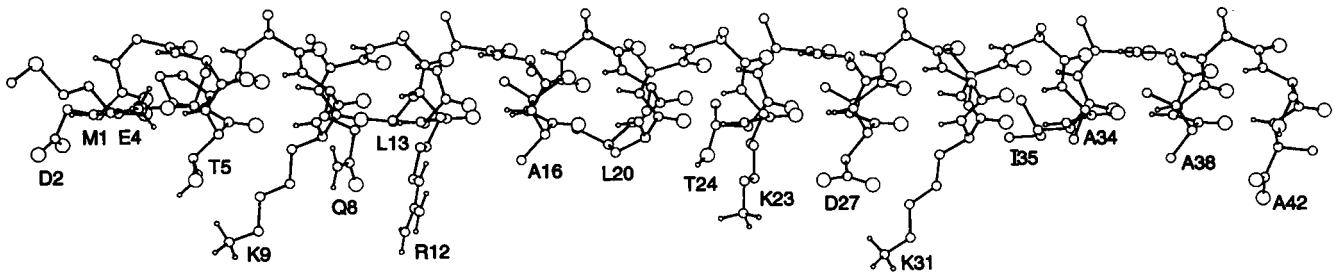

FIGURE 3 Side view of shorthorn sculpin AFP with labeled residues of the binding surface.

longer project into *a* axis cages. As a result, the methylene chains change configuration substantially in facilitating hydrogen bond formation. After minimization, the configurations of these side chains were found to depend sensitively upon the original position of the peptide. Other residues, including R12 and K23, also had variable interaction with ice, showing no obvious trend or pattern of binding. Interestingly, with the protein aligned along [−1 −2 2], side chains appeared to diverge from the backbone when viewed down the *c* axis such that no periodic grouping of side chains was seen (Fig. 4, *left*).

The precise fitting of the shorthorn sculpin AFP along [1 2 2] seemed to suggest a general structural match between the protein and the (2 −1 0) plane, which in itself may be an essential criterion for AFP binding. To assess structural accommodation of the bulk of the protein by ice, the [1 2 2] and the [−1 −2 2] binding scenarios were analyzed, visualizing only the van der Waals spheres of the α and β carbons of the AFP (Fig. 5). In this way the molecule was represented as a space-filling α-helix core, and the structural variability due to side chain positions was minimized. Fig. 5 reveals a striking compatibility between the structural core of the shorthorn sculpin AFP and the [1 2 2] direction topography of (2 −1 0) ice plane.

The AFP α-helix can be depicted as a series of four low-pitch right-handed spirals of β carbons of side chains protruding from its backbone (Fig. 5), such that every 11th residue falls approximately along a straight line, 16.9 Å apart. The spacing and direction of the spirals allow the bulk of the protein to align preferentially within the *c* axis grooves only when the protein is oriented along [1 2 2]. This "screw thread in groove" motif is not seen along [−1 −2 2]. Although the spacing of the spirals is consistent with the spacing of ice in this direction, the pitch of the spirals no longer directs the bulk of the protein into the accommodating ice grooves. Instead spirals cross nearly perpendicular to the deep *c* axis grooves, and the AFP offers a relatively flat, nonconforming binding surface to the ice. This simplified view of the protein also explains the arrangement of residue side chains seen above for the [1 2 2] direction binding. The alignment of β-carbon spirals with [1 2 2] allows the residues of the AFP binding surface (at four-residue intervals) to reside in the repeated ice *c* axis grooves while providing gaps between spirals to accommodate the ice ridges. Furthermore, the directions of the C_α-C_β bonds for the binding surface residues not only place their side chains into *c* axis grooves but also allow positioning of the side chains into *a* axis cages at the angles that provide their comfortable accommodation. This directional presentation of side chains allows even the methylenes of the lysine residues to fit comfortably into the ice without need of significant conformational change. The stretching of side-chain spirals across the *c* axis grooves seen along [−1 −2 2] allows for no periodic grouping of binding surface residues or compen-

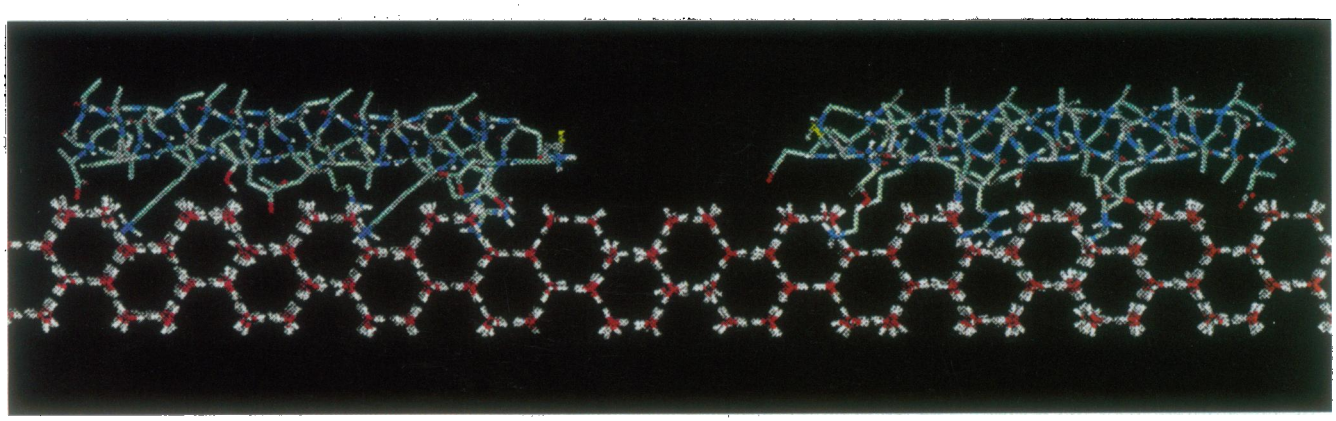

FIGURE 4 Shorthorn sculpin AFP on (2 -1 0) along [1 2 2] (*right*) and [−1 −2 2] (*left*). Both are viewed down the *c* axis at a 62° angle to the axis of the α-helices.

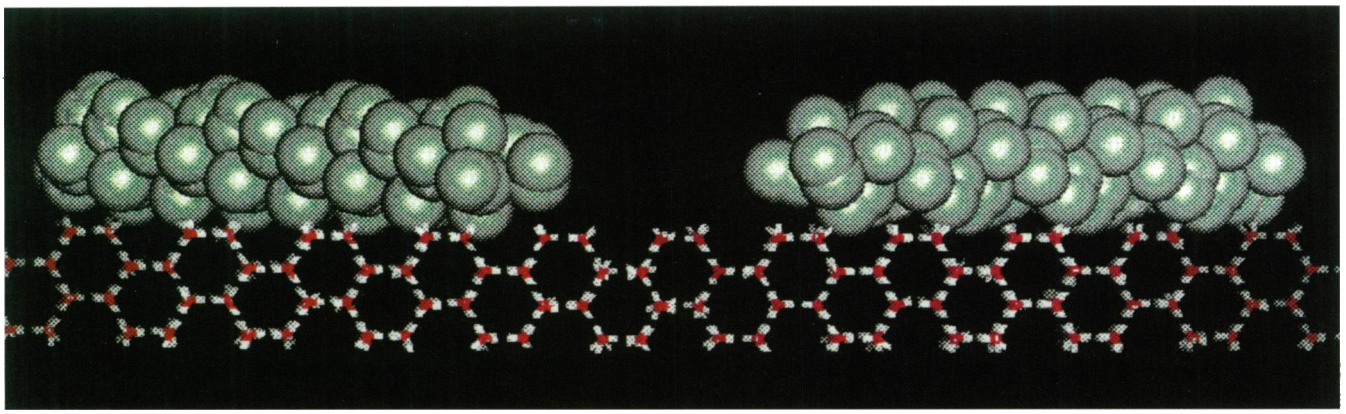

FIGURE 5 Structural match of shorthorn sculpin AFP on (2 −1 0) along [1 2 2] (*right*) and [−1 −2 2] (*left*) viewed down the *c* axis. Position of shorthorn sculpin AFP is the same as in Fig. 4, except here only van der Waals sphere representations of α and β carbons are shown and side chains are left off.

satory gaps between spirals. In this direction, the C_α-C_β bond directions appear to radiate side chains away from the backbone, not only preventing their alignment within *c* axis grooves, but also requiring substantial adjustment of their conformations to accommodate them in the ice surface. It is also important to note that rotation of the protein about the helix axis does not change the associations between the protein core (α and β carbons) and the ice surface as described above.

Based on our initial modeling results and previous suggestions that type I AFPs and AFGPs may adsorb to ice by becoming incorporated into its structure (Knight et al., 1993), an alternative binding scheme was considered for the protein along [1 2 2]. The presence of tetrahedral end groups on certain regularly spaced polar and/or charged residues along the shorthorn sculpin-binding surface suggests a possible mechanism in which these groups substitute for water molecules within the ice lattice. Thus, key initial hydrogen bonding could occur in register with the regular ice topography rather than within ice cages, because the two structures have the same translational spacing. The lysine NH_3^+ groups are strong candidates for this means of binding. The spacing of the three shorthorn sculpin AFP lysines puts them in nearly optimal positions to substitute for waters in the ice lattice, and their capacity for tetrahedral hydrogen bonding allows them to mimic such bonding within the ice and be naturally included in the crystal. This binding motif was tested by slightly shifting the AFP molecule already aligned along [1 2 2] and positioning the NH_3^+ of each lysine into the spot occupied by an appropriately oriented water molecule. Other binding surface residues of AFP were allowed to fit into ice cages as before. The three displaced waters were then deleted from the coordinate file and the system was minimized. Because no major change in the overall position of the protein backbone was required, structural conformity of the AFP and the ice as seen above was preserved. This version of the AFP-ice system yielded a binding energy of −616 kcal/mol, nearly equivalent to the binding energy attained with the complete ice surface. This binding of AFP revealed a uniform incorporation of the lysine NH_3^+ groups into the ice surface with complete tetrahedral hydrogen bonding (Fig. 6). Threonines were also considered for substitution, offering tetrahedral side chains with favorable hydroxyl groups; however, they did not provide unambiguous sites of water replacement in this binding position. Furthermore, the threonines have relatively short side chains, requiring that the protein backbone be very near the ice surface for direct hydroxyl substitution (Sicheri and Yang, 1995). As a result, longer binding surface side chains, especially those of lysines and arginine, were difficult to accommodate within the (2 −1 0) surface. Because of its suitable position, R12 would have preferentially been substituted for water in a manner analogous to that of K23, but R12 lacks a terminal tetrahedral group on

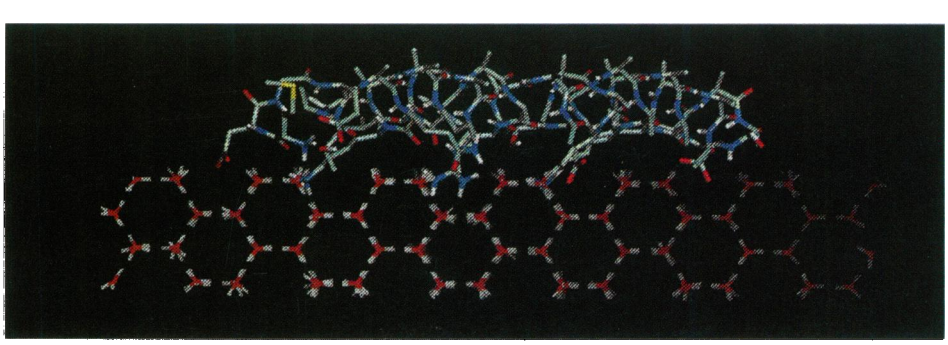

FIGURE 6 Shorthorn sculpin AFP minimized on (2 −1 0) along [1 2 2] viewed down the *c* axis with K9, K23, and K31 substituted for water molecules. Compare with the right side of Fig. 4.

its side chain. The participation of such charged or polar residues with planar end groups is unclear for this type of substitution mechanism. Fig. 7 shows the energy-minimized positions of binding surface residues with lysine substitution, illustrating the incorporation of lysines (blue) and the accommodation of principally hydrophobic side chains (green) within the *c* axis grooves. R12 is represented here in purple to denote its general position, although its exact interaction with the ice surface was not determined. Inspection of hydroxyl-containing residues T5, T24, and S41 (red) reveals a fairly regular array but no obvious pattern of binding. Of possible importance is the observation that T5 assumed the position of a water molecule, not within the given ice structure, but within the next level of waters that would normally be added to (2 −1 0) upon further ice growth. This suggests the possible incorporation of both lysines and threonine(s) into the regular hydrogen bonding pattern of the ice crystal at different levels of the surface. It is also worth mentioning that the importance of lysine groups for shorthorn sculpin binding was demonstrated experimentally: chemical modification of amino groups of the lysines of the shorthorn sculpin AFP leads to loss of its antifreeze activity (Cheng and DeVries, 1991).

To analyze the importance of the contoured fit of AFP protein to the ice topography, as seen in the shorthorn sculpin binding mechanism, we investigated another type I AFP from winter flounder on which extensive study and molecular modeling has been conducted (Knight et al., 1991; Wen and Laursen, 1992; Madura et al., 1994). Previous modeling of this protein verified its preferential binding along the [−1 1 2] direction of the (2 0 1) plane, as suggested by Knight et al. (1991), which is parallel to [1 2

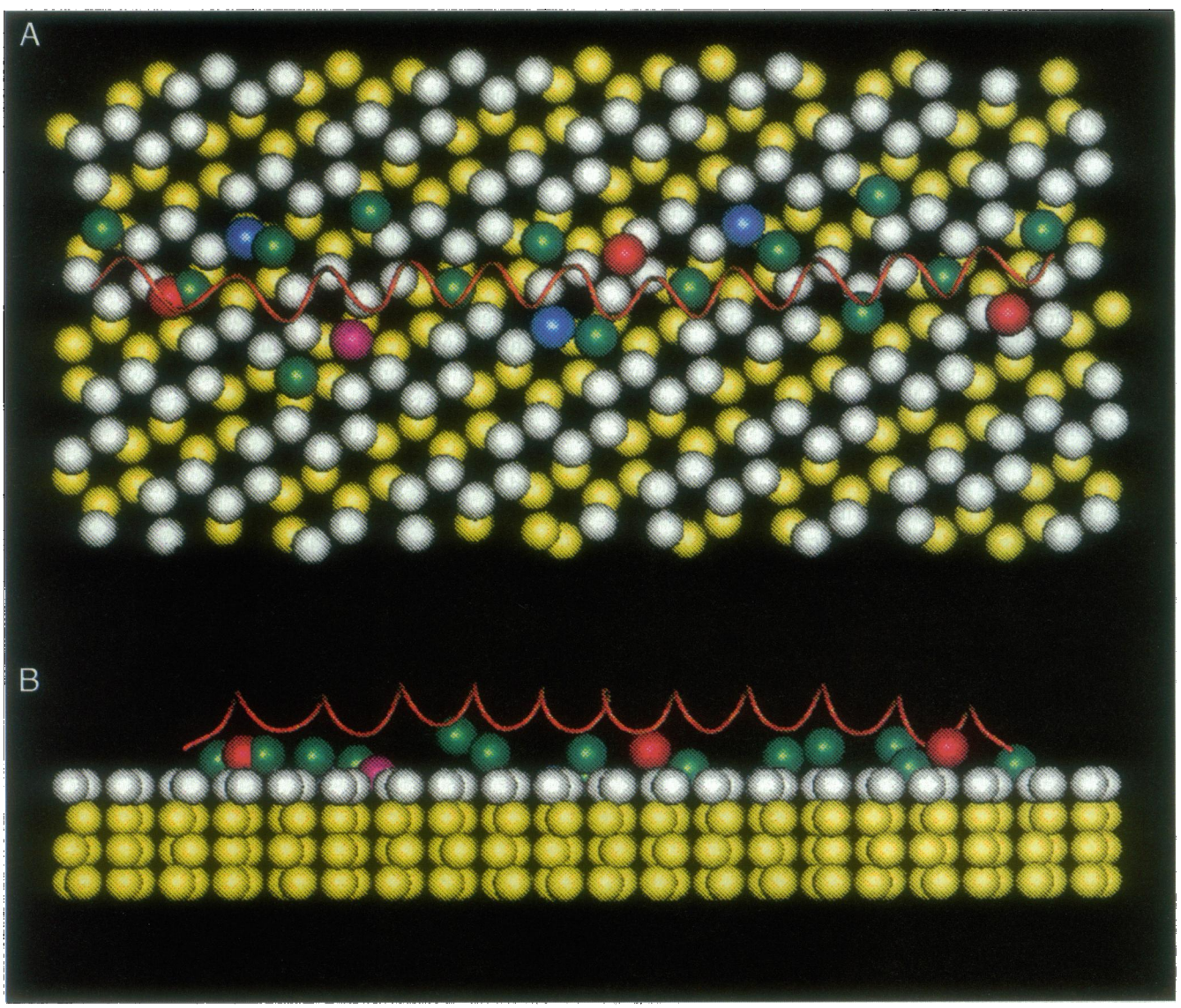

FIGURE 7 (*a*) Schematic top view of shorthorn sculpin AFP minimized along [1 2 2] direction on (2 −1 0), showing binding surface residues and the backbone helix (red). Blue, lysines; purple, arginine; red, threonines/serine; green, others. Note lysine substitution into the surface oxygen position. See text for the detailed discussion of binding. The binding position of shorthorn sculpin AFP is the same as in Fig. 6. (*b*) Side view of *a*.

2] of the (2 −1 0) plane. The (2 0 1) surfaces are bipyramidal planes, intersecting the *c* axis at oblique angles, compared to (2 −1 0) planes that are parallel to the *c* axis. The (2 0 1) planes are composed of areas of prism plane with regularly spaced steps. The winter flounder AFP takes advantage of regularly spaced T residues along its binding surface that bind to the outer corners of these steps. Because the binding groups in the winter flounder AFP do not protrude significantly, this binding optimizes the contact between the charged/polar residues and the ice surface. The large difference between winter flounder and shorthorn sculpin binding energy (−282 kcal/mol and −608 kcal/mol, respectively) is mainly due to the strong interaction with ice afforded by the charged residues of shorthorn sculpin AFP, particularly K9, R12, K23, and K31. Minimization of the repulsion between the protein backbone and nonbonding side chains with the ice is achieved via a contoured fit of the protein into *c* axis grooves of the (2 0 1) surface. Winter flounder AFP binding was compared to that of shorthorn sculpin AFP by viewing them simultaneously down the *c* axis of ice. The two proteins were represented by their backbones and respective β carbons to reduce them to space-filling models and eliminate side-chain variability. Fig. 8 illustrates the binding of these two type I AFPs, showing contoured fit of their backbones and side chains to their binding planes of ice.

Molecular dynamics

The molecular modeling presented in this paper was performed by using the idealized α-helix structure of the shorthorn sculpin, based on the assumption that the idealized AFP I peptide structure does not differ significantly from the structure obtained from molecular dynamics simulation in aqueous solution (Jorgensen et al., 1993; McDonald et al., 1993). Our comprehensive molecular dynamics studies of shorthorn sculpin in aqueous solution fully support this assumption. The results of the molecular dynamics simulation of the shorthorn sculpin AFP in water are shown in Figs. 9-11. Fig. 9 shows that there was no drift in the various energy components of the protein-water system during the last 84 ps of simulation time. The size of fluctuations for the potential energy and kinetic energy terms is consistent with similar simulations of type I AFPs in water (Jorgensen et al., 1993; McDonald et al., 1993). Fig. 10 shows the RMS difference from the idealized α-helix starting structure for shorthorn sculpin. In all four plots the RMS difference fluctuated about an average value for the last 84 ps of the simulation. This resulted in an overall average solution structure that was not significantly different from the idealized α-helical structure, as is illustrated in Fig. 11. The main structural deviation occurred in the N-terminus region after the proline residue. This deviation does not effect the placement of the residues and their side chains, which are involved in the recognition and binding of the shorthorn sculpin AFP to ice. It is interesting to compare the N-terminus region of the shorthorn sculpin AFP for the idealized α-helical structure and the average solvated structure obtained from molecular dynamics. For the former, the helical integrity at the N terminus appeared to be maintained partly by the electrostatic interaction between the amino terminal NH_3^+ of M1 and the COO^- of E4. The average dynamics structure showed the first four residues of the N-terminus region, namely M, D, G, and E, unfolded from the α-helical structure. Remarkably, starting with the T5 residue, the protein structure was almost perfectly α-helical.

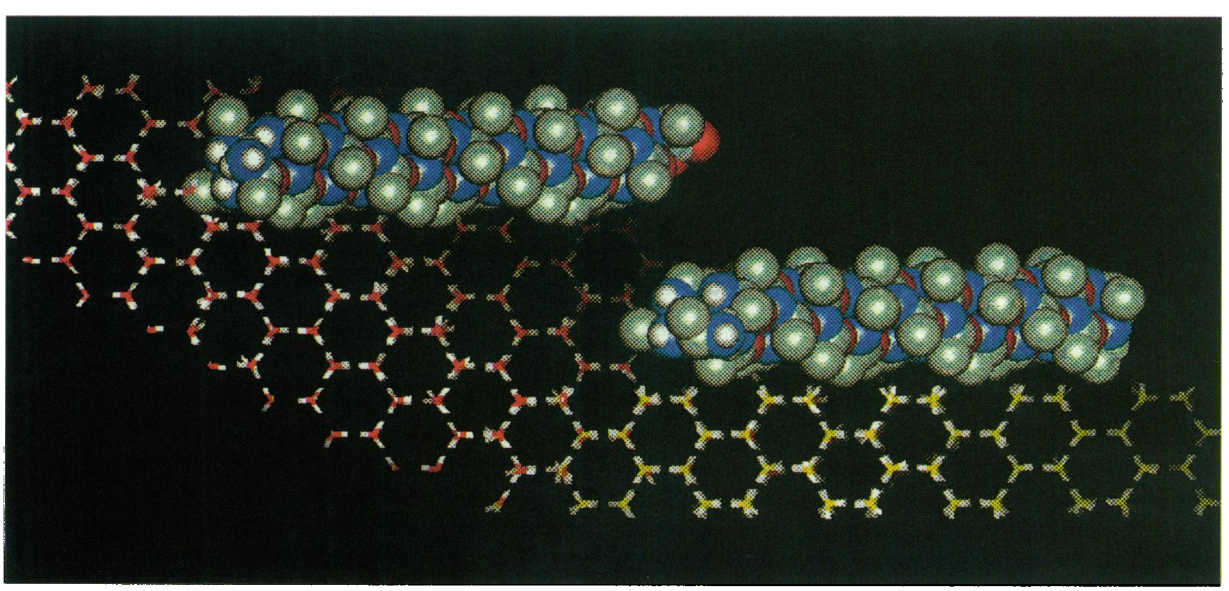

FIGURE 8 Structural fit of winter flounder AFP to (2 0 1) (red oxygens) and shorthorn sculpin AFP to (2 −1 0) (yellow oxygens) surfaces. Both are van der Waals radii representations of their protein backbones and β carbons. The (2 0 1) and (2 −1 0) surfaces are matched along the symmetry equivalent oxygen positions on both surfaces. Viewed down the *c* axes of the surfaces.

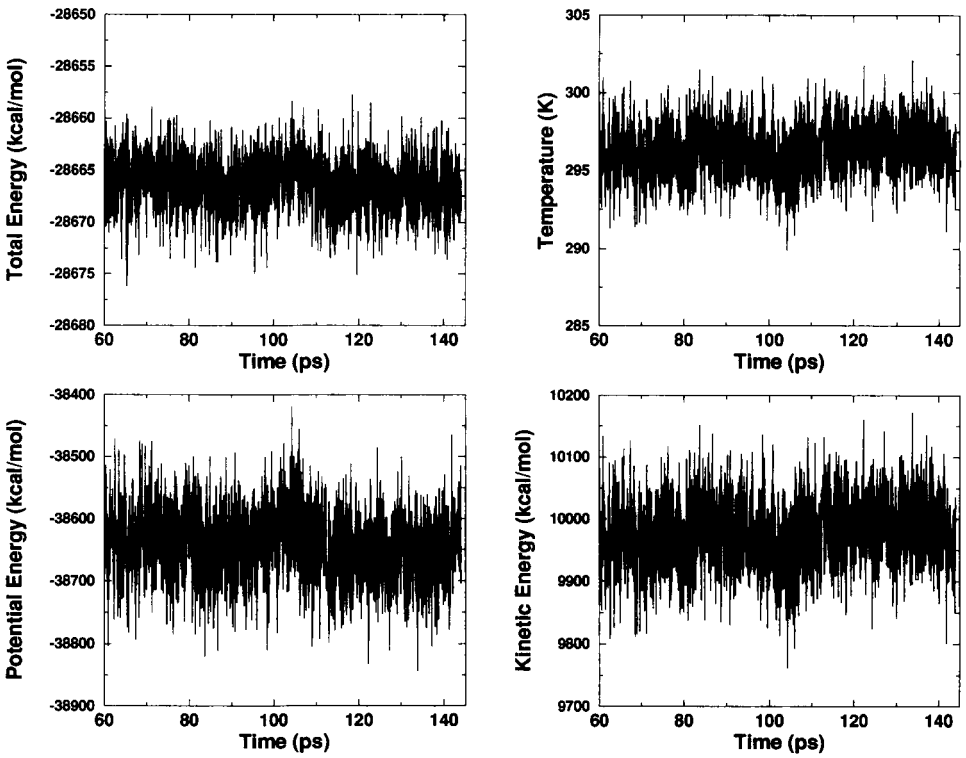

FIGURE 9 Plots showing the changes in (*a*) total energy, (*b*) temperature, (*c*) potential, and (*d*) kinetic energy for the last 84 ps of the molecular dynamics simulation. The data presented here were obtained during the data collection phase of the simulation, where velocities were not rescaled.

The helical structure at this end of the protein was stabilized by three hydrogen bonds between E4-Q8, T5-K9, and P6-A10. The proline in the *trans* conformation at position 6 seemed to be important for stabilizing the conserved part of the helix. This may be consistent with the observation that when proline is found near the N terminus, it is believed to actually stabilize the helix (Schultz and Schirmer, 1988). Fig. 10, *c* and *d*, shows that the C_α and C_β atoms fluctuated slightly, which allowed the AFP to accommodate the appropriate lattice sites on the ice surface.

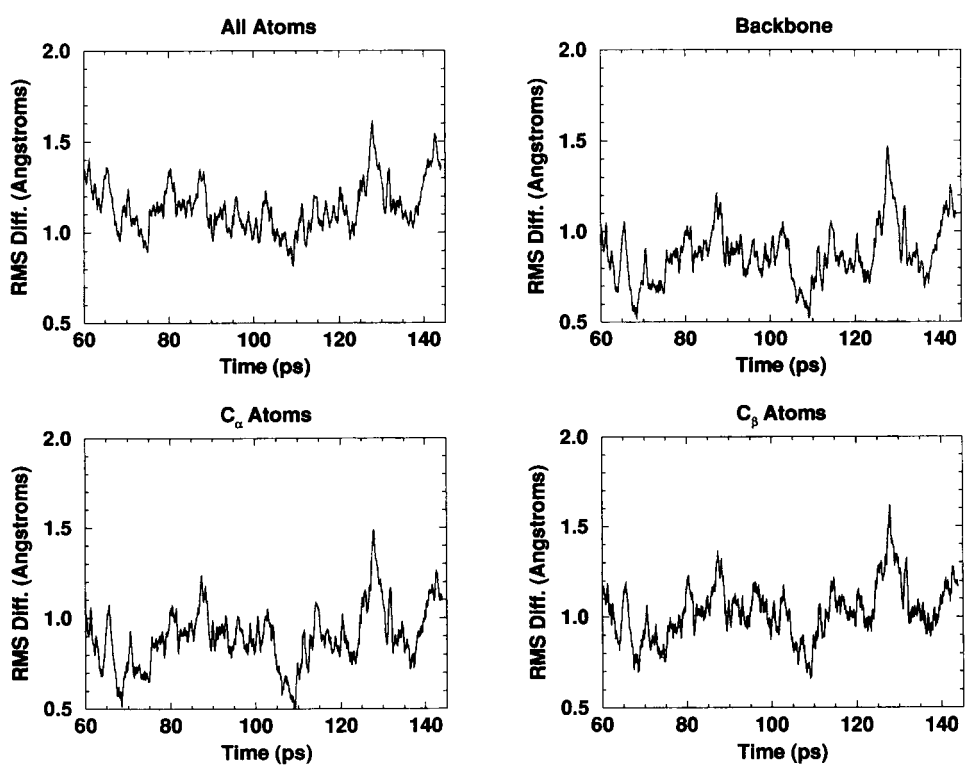

FIGURE 10 Plots of the RMS differences for the shorthorn sculpin from the last 84 ps. RMS differences for (*a*) all the atoms; (*b*) backbone atoms (N, C, O, and C_α) only; (*c*) C_α atoms; and (*d*) C_β atoms. These RMS differences were calculated using the idealized shorthorn sculpin as the reference structure.

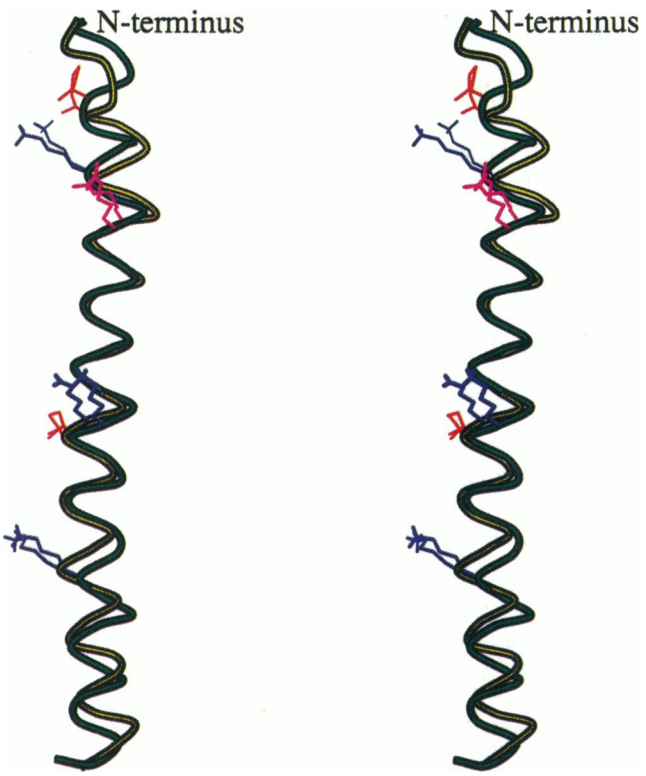

FIGURE 11 MOLSCRIPT (Kraulis, 1991) C_α stereo plot of the idealized shorthorn sculpin structure (green) superimposed on the averaged molecular dynamics structure (yellow). The lysine (blue), threonine (red), and arginine (purple) residues are represented as stick drawings.

To assess the effect of the dynamics simulation in aqueous solution on the shorthorn sculpin AFP structure, we reanalyzed the binding properties to the (2 −1 0) face of ice. As discussed earlier, the only significant structural changes were observed in the N-terminus region of the protein. The part of the protein that was essential for stereospecific binding was virtually unchanged during the dynamics. Binding analysis of the average, water-solvated dynamic structure of shorthorn scupin AFP along [1 2 2] revealed exactly the same features as discussed earlier for the idealized α-helical structure—that is, the favorable spacing of lysine residues, the fitting of the α-helical shape of the protein to the topography of ice, and the favorable positioning of threonines were again the key features of the recognition and binding process.

Interestingly, although the stereospecificity of binding to ice remained unchanged, the water-solvated, average dynamics structure of the shorthorn sculpin AFP had a binding energy of −665 kcal/mol along the [1 2 2] direction. This represented an increase in binding energy when compared to the binding energy along [1 2 2] of the ideal helix (−608 kcal/mol), which could be most likely attributed to two main factors. First, the N terminus of the protein released from the α-helix structure became involved in nonstereospecific binding to ice. Second, because of the fact that the hydrophobic part of the C-terminus region was bent slightly upward in the water-solvated structure of the protein, the repulsion between the protein and ice was reduced, again resulting in greater binding energy. It was interesting to observe that upon binding to ice, the helicity of the protein was substantially improved, showing template-like induced ordering of the protein backbone during the minimization process.

The binding energy of −507 kcal/mol of the solvated, shorthorn sculpin protein along the mirror-related direction [−1 −2 2] on (2 −1 0) was similar to the binding energy of −530 kcal/mol of the ideal α-helix along this direction. In this case the difference in binding energy along [−1 −2 2] of the solvated structure when compared to the ideal helix case was mainly due to the difference in the interactions formed between the N-terminus region of the protein and ice.

CONCLUSION

Ice etching, modeling, and energy minimization show the tendency for shorthorn sculpin AFP to bind preferentially along the [1 2 2] vector of the secondary prism (2 −1 0) faces of ice (Knight et al., 1991). Favorable binding energies and a structural match with the ice topography distinguish [1 2 2] and not its mirror image [−1 −2 2] as the unique direction of binding. Further inspection of our model reveals a general structural match between the protein and the ice surface when the protein is oriented along [1 2 2]. This complementarity is found to derive from the right-handed helical character of the AFP, which allows the repetitive low-pitch spirals of side chains formed by every fourth residue (represented by their β carbons in Fig. 5) to fit within the ice topography and align certain hydrophilic groups for hydrogen bonding. Further complementarity is seen in the projection of side-chain C_α-C_β bonds from the AFP backbone, which direct side chains into accommodating ice surface cages. Specific interaction of the protein with the ice surface appears to be based on the spacing of K9 and K31 (33.8 Å) as well as R12 and K23 (16.9 Å). Two binding models are proposed, the first requiring accommodation of binding surface residues within ice cages, and the second involving the inclusion of lysine side chain tetrahedral groups into the ice lattice. Both scenarios have favorable binding energies. Determination of explicit positioning and function of each AFP residue is beyond the scope of this study but should be undertaken with the availability of a full dynamic model of shorthorn sculpin AFP at a complete ice/water interface. The structure and binding of shorthorn sculpin AFP are compared to that of the winter flounder AFP, indicating the importance of the contoured fit of the protein into ice surface topography. Finally, the structure and binding properties of the shorthorn sculpin protein obtained from the molecular dynamics simulations in aqueous solution were compared to the idealized α-helical protein structure and binding. This analysis revealed great similarities in the structures of the protein in both cases,

except for a short section of the N-terminus region, and essentially the same mechanism of stereospecific recognition and binding to the ice surface.

In closing, it is worth mentioning that the stereospecific modification of crystal growth by proteins, polypeptides, or molecules to serve specific functions in organisms extends beyond the class of APF/AFPG molecules. Inhibition of crystal growth and crystal morphology modification are widely used in biomineralization processes in many organisms (Addadi and Weiner, 1992). Recently we have investigated stereospecific modification of calcite by oyster shell proteins and polyaspartate (Wierzbicki et al., 1994) and calcium oxalate monohydrate inhibition by citrate and phosphocitrate (Wierzbicki et al., 1995). Interactions of ionic inhibitors with ionic crystals are strong electrostatic-type interactions, in contrast to weaker, predominantly hydrogen-bond based interaction between AFPs and ice; nevertheless it seems that the same general principle of stereospecific modification of crystal growth at the molecular level is utilized in these two vastly different classes of biological systems.

This work was supported by grants from the National Science Foundation (MCB-9322602, EHR-9108761) and NOAA-Sea grant (NA16RG0155). The National Center for Atmospheric Research is funded by the National Science Foundation.

REFERENCES

Addadi, L., and S. Weiner. 1992. Control and design principles in biological mineralization. *Angew. Chem. Int. Ed. Engl.* 31:153–169.

Brooks, B. R., R. E. Bruccoleri, B. D. Olafson, D. J. States, S. Swaminathan, and M. Karplus. 1983. CHARMM: a program for macromolecular energy minimization and dynamics calculations. *J. Comput. Chem.* 4:187–217.

Cheng, C. C., and A. L. DeVries. 1991. The role of antifreeze glycopeptides and peptides in the freezing avoidance of cold-water fish. *In* Life Under Extreme Conditions. Guido di Prisco, editor. Springer-Verlag, Berlin, Heidelberg. 1–14.

Davies, P. L., and C. L. Hew. 1990. Biochemistry of fish antifreeze proteins. *FASEB J.* 4:2460–2468.

Duman, J. G., D. W. Wu, T. M. Olsen, M. Urrutia, and D. Tursman. 1993. Thermal-hysteresis proteins. *In* Advances in Low Temperature Biology, Vol. 2. JAI Press, Greenwich, CT. 131–182.

Hew, C. L., and D. S. C. Yang. 1991. Protein interaction with ice. *Eur. J. Biochem.* 203:33–42.

Jorgensen, H., M. Mori, H. Matsui, M. Kanaoka, H. Yanagi, Y. Yabusaki, and Y. Kikuzono. 1993. Molecular dynamics simulation of winter flounder antifreeze protein variants in solution: correlation between side chain spacing and ice lattice. *Protein Eng.* 6:19–27.

Jorgensen, W. L., J. Chandrasekhar, J. D. Madura, R. W. Impey, and M. L. Klein. 1983. Comparison of simple potential functions for simulating liquid water. *J. Chem. Phys.* 79:926–935.

Knight, C. A., C. C. Cheng. and A. L. DeVries. 1991. Adsorption of α-helical antifreeze peptides on specific ice crystal surface planes. *Biophys. J.* 59:409–418.

Knight, C. A., E. Driggers, and A. L. DeVries. 1993. Adsorption to ice of fish antifreeze glycopeptides 7 and 8. *Biophys. J.* 64:252–259.

Kraulis, P. 1991. MOLSCRIPT: a program to produce both detailed and schematic plots of protein structures. *J. Appl. Crystallogr.* 24:946–950.

Laursen, R. A., D. Wen, and C. A. Knight. 1994. Enantioselective adsorption of the D- and L- forms of an α-helical polypeptide to the {20–21} planes of ice. *J. Am. Chem. Soc.* 116:12057–12058.

Madura, J. D., A. Wierzbicki, J. P. Harrington, R. H. Maughon, J. A. Raymond, and C. S. Sikes. 1994. Interaction of the D and L forms of winter flounder antifreeze peptide with the (201) planes of ice. *J. Am. Chem. Soc.* 116:417–418.

McDonald, S. M., J. W. Brady, and P. Clancy. 1993. Molecular dynamics simulations of a winter flounder "antifreeze" polypeptide in aqueous solution. *Biopolymers.* 33:1481–1503.

Raymond, J. A., and A. L. DeVries. 1977. Adsorption inhibition as a mechanism of freezing resistance in polar fishes. *Proc. Natl. Acad. Sci. USA.* 74:2589–2593.

Schultz, G. E., and R. H. Schirmer. 1988. Principles of Protein Structure. Springer-Verlag, New York.

Sicheri, F., and D. S. C Yang. 1995. Ice-binding structure and mechanism of an antifreeze protein from winter flounder. *Nature.* 375:427–431.

Wen, D., and R. A. Laursen. 1992. A model for binding of an antifreeze polypeptide to ice. *Biophys J.* 63:1659–1662.

Wierzbicki, A., C. S. Sikes, J. D. Madura and B. Drake. 1994. Atomic force microscopy and molecular modeling of protein and peptide binding to calcite. *Calcif. Tissue Int.* 54:133–141.

Wierzbicki, A., C. S. Sikes, J. D. Sallis, J. D. Madura, E. D. Stevens, and K. L. Martin. 1995. Scanning electron microscopy and molecular modeling of inhibition of calcium oxalate monohydrate crystal growth by citrate and phosphocitrate. *Calcif. Tissue Int.* 56:297–304.